J_ID: Z3T Customer A_ID: MRM22619 Cadmus Art: MRM22619 Ed. Ref. No.: 10-11431.R2 Date: 30-August-10 Stage: Page: 1

FULL PAPER

Magnetic Resonance in Medicine 000:000–000 (2010)

Ex Vivo High Resolution Magic Angle Spinning Metabolic Profiles Describe Intratumoral Histopathological Tissue Properties in Adult Human Gliomas

A. Croitor Sava,[1]* M. C. Martinez-Bisbal,[2,3] S. Van Huffel,[1] J. M. Cerda,[4] D. M. Sima,[1] and B. Celda[2,3]

In gliomas one can observe distinct histopathological tissue properties, such as viable tumor cells, necrotic tissue or regions where the tumor infiltrates normal brain. A first screening between the different intratumoral histopathological tissue properties would greatly assist in correctly diagnosing and prognosing gliomas. The potential of ex vivo high resolution magic angle spinning spectroscopy in characterizing these properties is analyzed and the biochemical differences between necrosis, high cellularity and border tumor regions in adult human gliomas are investigated. Statistical studies applied on sets of metabolite concentrations and metabolite ratios extracted from 52 high resolution magic angle spinning recordings coming from patients with different grades of glial tumors show a strong correlation between the histopathological tissue properties and the considered metabolic profiles, regardless of the malignancy grade. The results are in agreement with the pathology obtained by the histopathological examination that succeeded the high resolution magic angle spinning measurements. The metabolite concentration set can better differentiate between the considered histopathological tissue properties compared to the ratios. Representative reference tissue models describing the metabolic behavior are extracted for characterizing the intratumoral tissue properties. The proposed metabolic profiles reflect that the metabolites behavior is interconnected, and typical biochemical patterns emerge for each histopathological tissue property. Magn Reson Med 000:000–000, 2010. © 2010 Wiley-Liss, Inc.

Key words: ex vivo; histopathological tissue properties; high cellularity; HR-MAS; infiltration; necrosis; tumor microheterogeneity

Glial brain tumors are one of the most common brain tumors found among adults. They are characterized by an extensive heterogeneity. This is reflected both at the level of the tumor type and grade, as well as at a microscale level, since along with viable tumor cells there may be necrotic regions. Moreover, glial tumors are highly infiltrative. Therefore, there may also be a contribution from normal brain tissue at the border of the affected area. These characteristics have posed serious difficulties in the diagnosis and prognosis of glial tumors. As a result, many researchers are now focusing on understanding this disease from the metabolomic, genomic and proteomic points of view.

Nuclear magnetic resonance (NMR) spectroscopy techniques, such as in vivo magnetic resonance spectroscopy (MRS) and ex vivo high-resolution spectroscopy, offer a clinically feasible metabolic assessment, providing significant biochemical information on the molecules of the organism under investigation. The potential of ex vivo and in vivo NMR spectroscopy has lately been extensively exploited in the separation between normal brain and brain tumors (1,2), as well as for the characterization of different degrees of malignancy (3–6). The focus in most of the previous studies lies mainly on brain tumor characterization and typing, without describing the histopathological tissue properties at a microscale level. However, there is an increasing interest in determining the correlation between metabolic features derived from ex vivo high resolution magic angle spinning (HR-MAS) and histopathological properties, as the HR-MAS technique is becoming a metabolomic methodology with potential applications in supporting tumor classification and diagnosis. Previous studies have shown that HR-MAS can help in predicting the growth characteristic within different regions of a tumor (7) and can help in differentiating between glial tumor grades (6). Moreover, with HR-MAS one can successfully reveal the status of tumor microheterogeneity (8) and can observe tumor metabolic alterations before they are morphologically detectable (9), which, in turn, can further be correlated to histopathological properties (3). Nevertheless, these studies limit themselves at describing independent metabolite behavior while ignoring their interconnectivity. Therefore we propose a multivariate statistical study

[1]Department of Electrical Engineering (ESAT), Division SCD, Katholieke Universiteit Leuven, Leuven, Belgium.

[2]Departamento de Química-Física, Facultad de Química, Universitat de Valencia, Valencia, Spain.

[3]CIBER-BBN, ISC-III, Universitat de Valencia, Valencia, Spain.

[4]Departamento de Patología, Facultad de Medicina, Universitat de Valencia, Valencia, Spain.

Grant sponsor: EU projects Etumour; Grant number: FP6-2002-LIFESCIHEALTH 503094; Grant sponsor: Research Council KUL: GOA Ambiorics, GOA MaNet; Grant number: CoE EF/05/006 Optimization in Engineering (OPTEC), IDO 05/010 EEG-fMRI, IDO 08/013 Autism, IOF-KP06/11 FunCopt; Grant sponsor: FWO; Grant number: G.0302.07, G.0341.07, G.0427.10N; Grant sponsor: IWT; Grant number: TBM070713-Accelero, TBM070706-IOTA3, TBM080658-MRI; Grant sponsor: Belgian Federal Science Policy Office; Grant number: IUAP P6/04, ESA PRODEX No 90348; Grant sponsor: EU; Grant number: (FP6-2002-LIFESCIHEALTH 503094), FAST (FP6-MC-RTN-035801); Grant sponsor: Neuromath; Grant number: COST-BM0601; Grant sponsor: Ministerio Ciencia e Innovación de España projects; Grant number: SAF2007-65473; SAF2007-29393-E; SAF2007-29394-E; SAF2007-29455-E; Grant sponsor: Ministry of Science and Innovation of Spain; Grant number: SAF2008-00270

*Correspondence to: Anca Croitor Sava, Departement Elektrotechniek, ESAT-SCD, Kasteelpark Arenberg 10, postbus 2440, B-3001 Leuven, Belgium. E-mail: anca.croitor@esat.kuleuven.be

Received 10 February 2010; revised 4 August 2010; accepted 6 August 2010.

DOI 10.1002/mrm.22619
Published online in Wiley Online Library (wileyonlinelibrary.com).

© 2010 Wiley-Liss, Inc.

J_ID: Z3T Customer A_ID: MRM22619 Cadmus Art: MRM22619 Ed. Ref. No.: 10-11431.R2 Date: 30-August-10 Stage: Page: 2

where sets of features coming from combinations of different metabolites and metabolite ratios are analyzed for assessing their relevance in correlating the HR-MAS spectra with the histopathological tissue properties.

Although HR-MAS is increasingly used to analyze tumor tissue biochemistry, nowadays histopathological analysis of the surgically extracted tumor tissue is usually considered as the gold standard for assigning the type and grade of the tumor, as well as the contribution of necrosis, high cellularity and normal brain tissue within the tumor area. Since HR-MAS spectra are obtained directly from the biopsy sample, HR-MAS can reveal a first level of correlation between metabolic profiles and biopsy tissue type, allowing for a better investigation of the tumor. Additionally, with ex vivo HR-MAS the tissue integrity is mostly conserved. This is a major advantage since it allows one to perform, on the same tissue sample, multimodal studies including subsequent genomic, proteomic or histopathological analyses and, therefore, to obtain a direct comparison between all these techniques. The added value of combining and comparing different techniques has been shown before (8–11). Such analyses, based on multiple data sources, can provide further insights into the biology of the brain tumors and improve the diagnosis.

In this study, we propose to further assess the correlation between metabolic features derived from ex vivo HR-MAS and necrosis, high cellularity or infiltration, which are common histopathological tissue properties. Therefore, both metabolomic and histopathological knowledge is considered. Compared to (8), where similar conclusions are drawn from tissue samples coming from the same patient, this work employs a multicenter database of frozen tissues extracted from 52 patients presenting different types of glial tumors [glioblastoma (GBM), grade III (GIII), and grade II (GII)].

The purpose of the study is threefold. (1) First, to analyze whether with unsupervised classification methods we can identify for each glial tumor the predominant histopathological tissue property. As the highest heterogeneity is observed and confirmed by the histological study in the GBM group, we first investigate this group. To this end, feature sets coming from various metabolites and metabolite ratios are tested as potential biomarkers for the considered clustering problem. The statistically significant correlation between the considered feature sets and the predominant histopathological tissue properties is also investigated. (2) Second, to extract representative reference metabolic tissue models for each histopathological tissue property and to analyze which of the considered input feature values are most sensitive in revealing the predominant histopathological property. (3) Finally, to test whether the conclusions drawn for the GBM group can be extended to other glial tumor groups, with different grade of malignancy.

MATERIALS AND METHODS

Data Acquisition

Brain tumor biopsies were carried out on 52 adult patients. Three hospitals provided the samples used in this study: Hospital La Ribera-Alzira (Valencia), Hospital Clínico Universitario (Valencia) and Instituto FLENI (Buenos Aires), all participating as partners in the eTUMOUR project (www.etumour.com). Initial diagnosis, done in each centre as a routine part for the standard patient management, assigns the considered cases to glial tumor group with different degree of malignancy: 27 grade IV glioblastoma tumor (GBM), seven grade III glial tumor (GIII), and 18 grade II glial tumor (GII). The tissue specimens were snap-frozen in liquid nitrogen and stored at -80°C until the time of spectroscopic analysis, when 1D PRESAT (pulse-and-acquire) data were acquired. HR-MAS experiments were conducted on 29/52 samples using a Bruker Avance DRX 600 spectrometer operating at a 1H frequency of 600.13 MHz. The instrument was equipped with a 4 mm triple resonance $^{1}H/^{13}C/^{15}N$ HR-MAS probe with magnetic field gradients aligned with the magic angle axis. Twenty-three of fifty-two samples underwent HR-MAS experiments using a Bruker Avance DRX 500 spectrometer operating at a frequency of 500.13 MHz. The instrument was equipped with a 4 mm triple resonance $^{1}H/^{31}P/^{13}C$ HR-MAS probe. A single-pulse 90° presaturation experiment was acquired in all the samples. Number of transients was 256 collected into 32 k data points for all the experiments. Water presaturation was used during 1 sec along the recycling delay for solvent signal suppression. Spectral width was 8 and 10 kHz for 600 and 500 MHz NMR spectrometers, respectively. To keep the rotation sidebands out of the acquisition window, samples were spun at 5000 Hz in the DRX 600 spectrometer and at 4000 Hz in the DRX 500 spectrometer. Sample temperature was kept at 4°C, using the cooling of the inlet gas pressures responsible for the sample spinning. Recycling delays were 1.5 sec for all experiments. Each sample was introduced in a 4 mm ZrO_2 rotor fitted with a 50-mL cylindrical insert, without any previous D_2O washing.

Histological Analysis

After performing the HR-MAS study, tumor specimens were snap-frozen and submitted for quantitative histopathological examinations. Thirty-seven of fifty-two biopsy samples (22 GBM, six GIII and nine GII) were subject to histological examination performed on tissue samples taken from the same part used in the HR-MAS study. The analysis was done by an expert neuro-pathologist and the samples were classified according to the revised WHO criteria (12). The samples were fixed in 10% formalin, embedded in paraffin, serially sectioned, slide mounted and stained with hematoxylin and eosine. Routine histological methodology has been used for evaluating the cell density and the percentage of necrosis. On the basis of the histology, the samples are considered with variable content of highly cellular tumor tissue, infiltrations with normal tissue and/or necrotic tissue. The percentage of tissue with a predominant property was calculated for each sample by measuring the total area of the biopsy sections and then delineating the regions of interest. Each case was assigned as having a certain histopathological tissue property when its corresponding region was $\geq$50% from the total area and any of the other two properties was observed in under 20%.

Author Proof

ID: jaishankarn | Black Lining: [ON] | Time: 21:40 | Path: N:/3b2/MRMT/Vol00000/100302/APPFile/JW-MRMT100302

J_ID: Z3T Customer A_ID: MRM22619 Cadmus Art: MRM22619 Ed. Ref. No.: 10-11431.R2 Date: 30-August-10 Stage: Page: 3

Nevertheless, for the largest part (~85%) of the high-cellularity samples, the histology post-HR-MAS showed a percentage of cellularity ≥75%.

Data Processing

The HR-MAS spectra were preprocessed as follows. Signals were truncated from 8120 points to the first 2048 points to reduce the computational load in the preprocessing steps. The water components were removed by HLSVD-PRO (13). Contributions outside the frequency interval [0.25, 4.2] ppm were filtered out to keep only the contribution of the metabolites of interest. Small variations in the chemical shift of peaks between HR-MAS experiments have been noticed. Therefore, all filtered 1D PRESAT were aligned with respect to the alanine doublet at 1.47 ppm (14). Signals were then normalized (divided by the $l2$ norm of the frequency domain signal between 0.25 and 4.2 ppm). A baseline correction was applied using an apodization function in the following way. The signal was point-wise multiplied in the time-domain with an exponentially decaying function. The resulting spectrum then mainly contained the broad baseline components, which were subsequently subtracted from the original spectrum, yielding the preprocessed signal.

Statistical Analysis

Sets of metabolite features were tested along with metabolite ratio feature sets to determine which is most likely to preserve the tissue's histological information. As relevant biomarkers for our study we considered total lipids group (Lips), *N*-acetylaspartate (NAA), Creatine (Cr), total Choline group (tCho). Peak integration was used for extracting the concentration of these metabolites by considering the following integrated intervals in ppm: Lip1 [0.84, 0.91], Lip2 [1.255, 1.285], Lip3 [2.79, 2.81], NAA [2.0, 2.015], Cr [3.01, 3.03], Cho [3.19, 3.205], PCho [3.21, 3.22], GPCho [3.225, 3.235]. These areas were computed from the mean of all the available HR-MAS spectra. Specifically, the highest point in the area to be integrated was identified for each metabolite, then the area bounds were fixed for each metabolite individually to those ppm values at which peak slopes return to baseline, but keeping symmetric intervals with respect to the highest point. The ratio set was composed of Lips, NAA, and tCho with respect to Cr. Hence, the considered features were real-valued numbers that can be represented as points in an n-dimensional space, where $n = 7$ for the concentrations case, and $n = 3$ for the ratios case. All the statistical techniques described below were applied exclusively to these feature vectors. The steps involved in the statistical analysis were: distribution analysis, clustering, and validation.

Data Distribution

For obtaining information about the location and the spread of the data we studied the variance within each tumor group by computing the median and the interquartile range. This representation is thus helpful to detect possible skewness in the data and existing outliers.

Data Clustering

Cluster analysis was used to determine if the considered feature sets have the potential to predict histopathological tissue properties. The *k*-means clustering algorithm (15) was applied to our data. Given a prespecified number k, the *k*-means algorithm partitions the data set into k subsets (clusters $C_1 \ldots C_k$) by iteratively optimizing the sum, over all clusters, of the within-cluster sums of object-to-cluster-centroid distances:

$$E = \sum_{i=1}^{k} \sum_{x \in C_i} d(x, \mu_i), \qquad [1]$$

where $d(x,\mu_i)$ is the distance between x, an object in cluster C_i, and μ_i, the centroid of C_i. Each centroid is the component-wise mean of all the objects (feature vectors) in that cluster, after centering and normalizing the sequence of values within each object to zero mean and unit standard deviation.

As we are interested in the similarity in shape between two feature vectors, the correlation distance was considered most appropriate for our data. More precisely, the distance $d(x,\mu_i)$ is computed as (16):

$$d(x, \mu_i) = 1 - \frac{(x - \overline{x})(\mu_i - \overline{\mu}_i)'}{\sqrt{(x - \overline{x})(x - \overline{x})'(\mu_i - \overline{\mu}_i)(\mu_i - \overline{\mu}_i)'}} \qquad [2]$$

where the bar denotes a vector with all elements equal to the mean of the values in the given vector, and the prime denotes vector transposition (here, x and μ_i are row vectors).

Statistical Validation

A critical parameter in clustering is the number of clusters, k. To minimize subjectivity when choosing the best number of clusters for our data, we estimate it with several statistical indices, which measure the quality of clusters on the basis of the definition that objects within one cluster are similar to each other, while objects in different clusters are dissimilar with each other. The optimal number of clusters among different values of k is obtained by evaluating the solutions of the following proposed validity indices: weighted inter–intra index (Wint) (17), Krzanovski-Lai index (KL) (18), silhouette index (Sil) (19), and Homogeneity and Separation index (20).

As a final measure of the statistical significance of our data analysis we estimate the cluster reliability, or the likelihood that the cluster structure is not formed by chance. For this, Tukey's multiple comparison (21) was considered after performing the Kruskal–Wallis test (22). This procedure provides a comparison interval for the mean value of the considered features allowing one to check if the metabolite alterations are statistically significant between the considered clusters. When the intervals overlap, there is no statistically significant difference in metabolite alterations within clusters, while if the intervals are disjoint, the difference can be considered as statistically significant.

J_ID: Z3T Customer A_ID: MRM22619 Cadmus Art: MRM22619 Ed. Ref. No.: 10-11431.R2 Date: 30-August-10 Stage: Page: 4

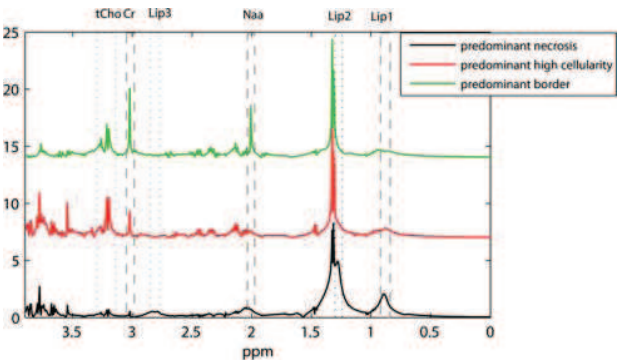


FIG. 1. HR-MAS spectra coming from GBM samples with different predominant tumor histopathological properties. The vertical lines highlight the region where the considered metabolites are located in ppm scale.

Correlation with Histopathology

After assigning each case to one of the clusters, we also look into the relationship of each cluster to histopathology. For labeling the clusters, the correlation between the cluster centroids μ_i and the metabolic profile coming from pure tissue samples (with the dominant histopathological tissue property more than 90% of the total region) is computed by means of correlation coefficients. Clusters were labeled considering the highest correlation coefficient value. Furthermore, reference metabolic models are proposed for necrotic, highly cellular and border tissue, by computing the mean of the feature vectors belonging to the same cluster after centering and normalizing the sequence of values within each feature vector to zero mean and unit standard deviation. Only the cases with histopathological confirmation were used in this step.

Grade II and Grade III Gliomas Tissue Characterization

One purpose of this study is to analyze to which extent the molecular composition is dependent on the tumor grade. To this end, the metabolomic analysis, supported by histopathology, was extended to the GII and GIII glioma groups. For each case within the GII and GIII tumor groups we computed the correlation coefficient between the feature vector extracted from the HR-MAS spectra and the reference models obtained for the GBM group in the previous step. This approach should give us further insight to whether the metabolic profiles from the GBM clusters change significantly with the tumor grade, and whether a similar molecular composition can be observed for necrosis, highly cellular or infiltrations, regardless of the grade of malignancy.

RESULTS

Results of the Statistical Analyses

According to the histological exam, a great extent of tissue heterogeneity is observed for all the studied glial tumors. The high grade tumors appear to be more heterogeneous than low grade tumors. In particular for the GBM group, although all cases within this group were initially diagnosed in the hospital as high grade GBM tumor, they are highly variable in their composition as different content of necrotic, high cellularity or infiltrations with normal tissue was reported by histopathology. Some samples contain 90–100% necrosis and some contain only areas of infiltrating tissue at the border of the tumor. The intergroup variability is reflected also at metabolic level (Fig. 1). The metabolite concentration distributions are observed to be widely dispersed around the median values and outliers can be identified. We investigate whether the identified outliers cluster together as a new subgroup within the GBM group. F1

Using no prior knowledge, data clustering of the GBM group in three subgroups is indicated as the best solution by the Homogeneity-Separation, Sil and Wint indices (see Fig. 2a and b). According to these findings, $k = 3$ is further considered the optimal number of clusters for the k-means clustering algorithm. KL index suggests four as the best number of subgroups for data clustering. F2

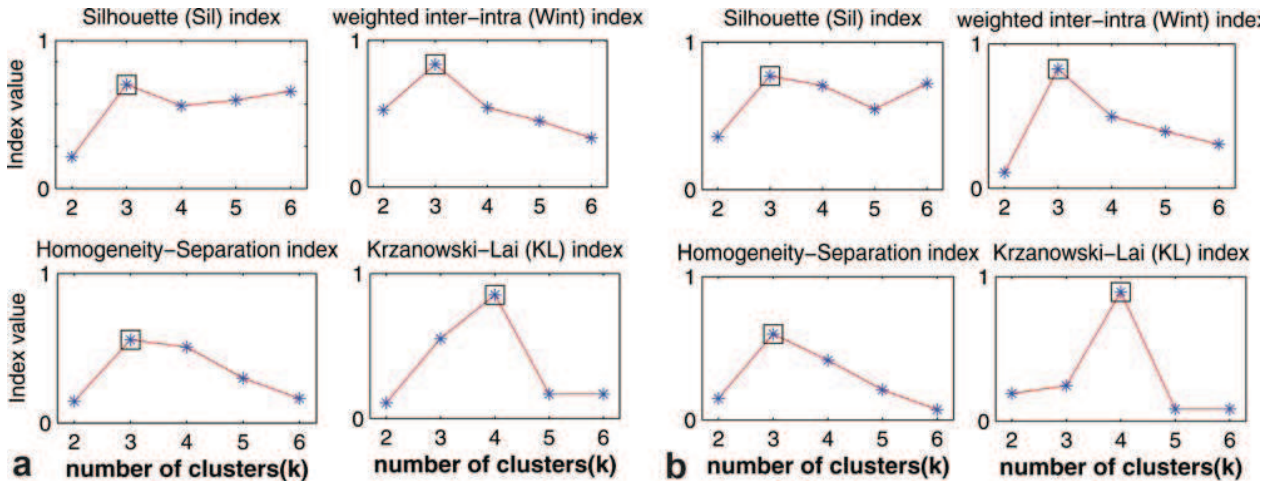


FIG. 2. Statistical indexes for estimating best k for k-means when considering (**a**) the metabolite concentrations as input features and (**b**) the metabolite ratios as input features. The highest index value, indicating the optimal number of clusters, is contoured with black squares.

ID: jaishankarn | Black Lining: [ON] | Time: 21:40 | Path: N:/3b2/MRMT/Vol00000/100302/APPFile/JW-MRMT100302

J_ID: Z3T Customer A_ID: MRM22619 Cadmus Art: MRM22619 Ed. Ref. No.: 10-11431.R2 Date: 30-August-10 Stage: Page: 5

COLOR

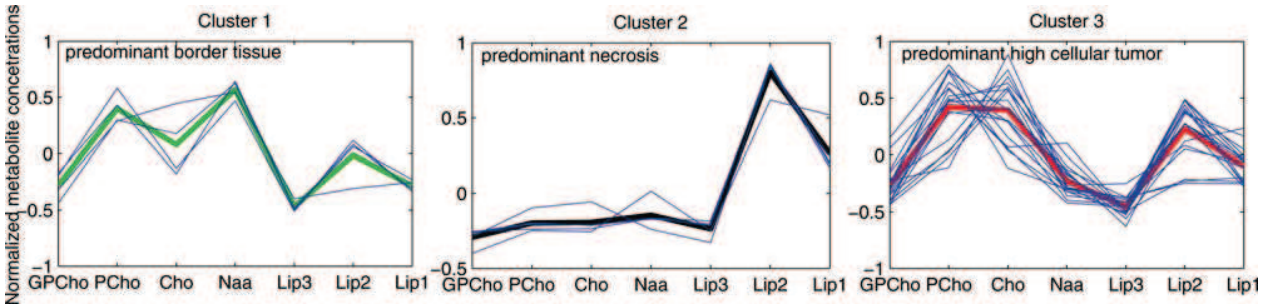


FIG. 3. Feature profiles of clusters for GBM samples: centroids are marked in bold, and objects within clusters are marked blue.

The fourth cluster contains in fact only one case, which was considered by histopathology with over 90% contributions from normal tissue. The results of the clustering F3 F4 procedure are presented in Figs. 3 and 4. We can visually observe considerably high differences in the metabolite profiles between the three clusters. The obtained clusters are homogeneous and clearly separable. μ_1 correlates best with infiltrative border tissue (corr = 0.84), μ_2 with the necrotic tissue (corr = 0.98) and μ_3 with the highly cellular tissue (corr = 0.85). Additionally, we assess the relationship between these findings and the conclusions drawn from histology. A very good agreement is obtained when working with the metabolite concentrations set, as 21 of 22 histopathologically validated cases were found to contain tissue with the same predominant histopathological property, both with HR-MAS clustering analysis and with the histopathological procedure. The results are in agreement with literature since μ_1 is characterized by high levels of NAA, which are typically found at the border region of the tumor or in regions with infiltrative normal tissue (23). μ_2 presents very high levels of Lip(s), which is an expected behavior for GBM tumors and is mainly associated with necrosis (3), while μ_3 has high level of Cho(s), a generally accepted biomarker of active tumor cell growth (24). We will further refer to the obtained clusters as border tissue (C_1), necrotic tissue (C_2) and high cellularity tissue (C_3), respectively. In Fig. 4, all the GBM cases projected in a multidimensional scaled plane represented by the first three principal coordinates (PCOs) (25), are showed. For case 3, indicated by a light blue circle in Fig. 4, an agreement between the metabolic and the histopathological analysis was not obtained. It was clustered as predominantly highly cellular tumor, while histology reports this area to be composed primarily of normal tissue. As this tissue type is not considered in our study, case 3 is reported as an outlier and this could explain its location outside the three obtained clusters. The same case was assigned by the KL index to a separate cluster. The five cases for which we do not have the histopathological validation (indicated by a dark green circle in Fig. 4) do not influence the clustering results, as they are evidently grouped with the other objects in their clusters.

When considering the metabolite ratios, an agreement with the histopathology was obtained for 18 cases out of 22. Three of the four cases without agreement cluster as predominantly border tissue when considering the ratios, while the histopathology reports a high percentage of active tumor cells. Case 3 was assigned, also when working with metabolite ratios, to predominantly highly cellular tumor tissue.

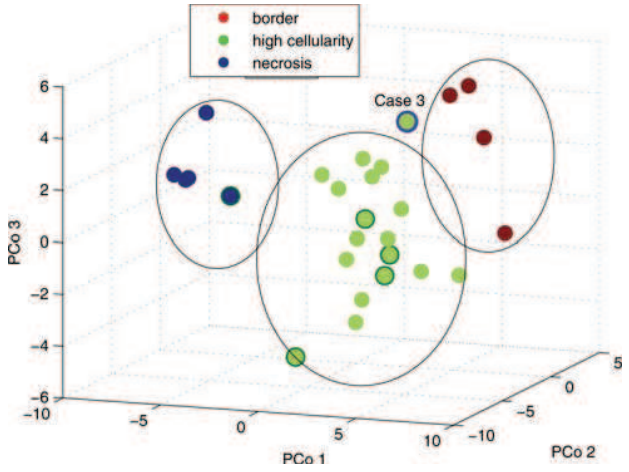


FIG. 4. Data visualization in the principal coordinates space. First three principal coordinates (PCoi) of GBM samples were considered. The three black ovals drawn on the obtained image encompass the clusters' population.

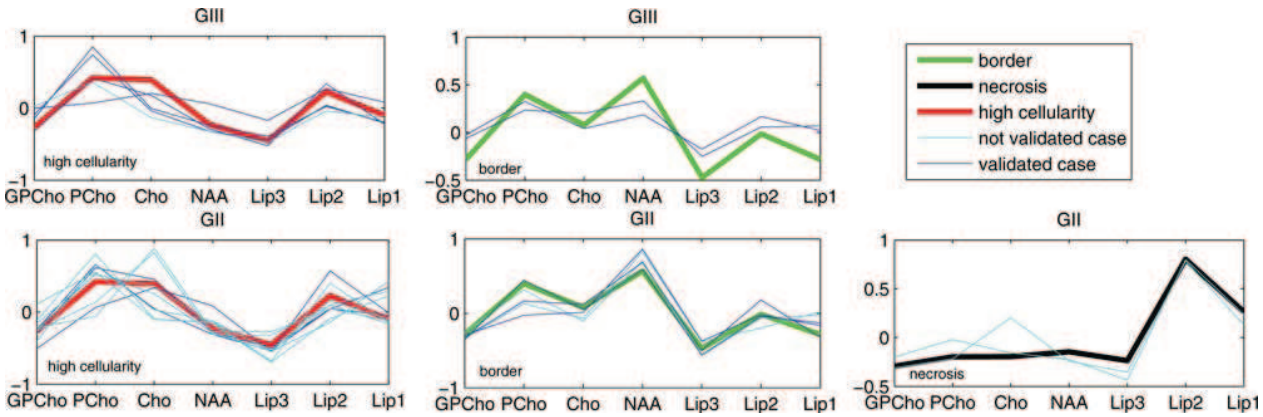
Grade II and Grade III Glioma Characterization

For the GIII tumor group, two cases out of seven are highly correlated with the border tissue model and five cases are highly correlated with the high cellularity tissue model, see Fig. 5. These results are in agreement F5 with the histology. A special situation is represented by case 28, for which the histopathology reveals equal percentage of highly cellular tumor tissue and infiltrations (50–50%). The metabolic profile of this case correlates AQ2 most with predominantly border tissue. Still, a very high correlation with the highly cellular tissue model is also obtained. No case with predominantly necrosis was reported for this tumor group.

For the GII tumor group, the metabolic analysis indicated that 11 cases were highly correlated with the highly cellular tumor tissue model, five cases with the border tissue model and two cases with the necrotic tissue model, see Fig. 5. A good agreement with the histology was obtained for seven out of the nine histopathologically validated cases. Histopathology confirms for one case within this tumor group some contributions from

ID: jaishankarn | Black Lining: [ON] | Time: 21:41 | Path: N:/3b2/MRMT/Vol00000/100302/APPFile/JW-MRMT100302

J_ID: Z3T Customer A_ID: MRM22619 Cadmus Art: MRM22619 Ed. Ref. No.: 10-11431.R2 Date: 30-August-10 Stage: Page: 6



C O L O R

FIG. 5. Assignments based on highest correlation coefficient within GIII and GII glial tumor group, respectively.

necrotic tissue. This apparent inconsistency (one grade II glioma presenting necrosis) could be a consequence of the fact the tissue sample analyzed with HR-MAS is not strictly coming from the same tumoral region as the one used for initial diagnosis. The two cases assigned by metabolic analysis to necrosis reveal high lipids levels. As in (3), lipids are observed to be present in non-necrotic biopsy samples. This could be, for example, due to hypoxia, since lipids may originate not only from regions of necrosis, but also from viable growth-arrested cells (26).

DISCUSSION

The present work illustrates a significant correlation between the tumor microheterogenity as revealed by the histopathology and ex vivo HR-MAS sets of metabolite concentrations and ratios. These findings could aid in a better understanding of glial tumor tissue metabolism, and therefore could improve in diagnosis and prognosis of the tumor type and grade.

Combinatorial approaches, where different techniques are correlated for assessing the relation between clinically relevant cell processes and specific metabolites, have been previously proposed. In (10) and (11), combining HR-MAS and genomic data provide insights into the biology of glial tumors. In (8) HR-MAS of intact brain tumor biopsies are combined with histopathology for revealing tumor microheterogeneity. Specifically, the concentration of mobile lipids and choline were reported to correlate linearly with the amount of necrosis and tumor cellularity, respectively, while higher levels of NAA are expected in the border region of the tumor with respect to the active tumor region. Still, the conclusions drawn in (8) are coming from a limited number of samples originating from a single patient with GBM tumor. We propose a more complex study where samples measured in different clinical centers and coming from different patients with glial tumor with different grades of malignancy are analyzed using advanced statistical methods. Our results confirm that, by using only information coming from ex vivo HR-MAS data, we can clearly differentiate between histopathological tissue properties within glial brain tumors, regardless of the malignancy grade. An important finding is that the alterations in metabolite concentrations are correlated and not independent from each other. Based on this, representative tissue models describing metabolites' behavior for necrotic, highly cellular and border tumor tissue can be derived. To our knowledge this is the first study that derives the metabolic profiles of the three considered histopathological tissue properties.

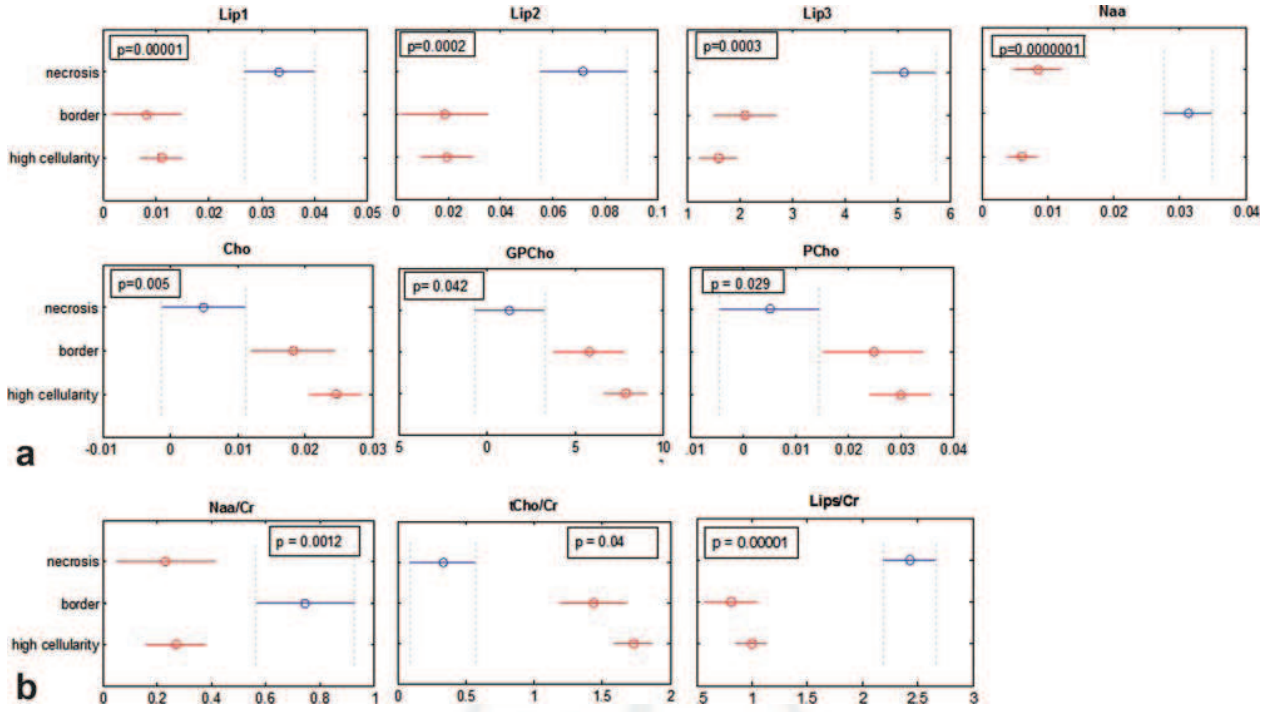
Best Biomarkers for Tissue Differentiation and Characterization

The results suggest that all the investigated metabolites and ratios are sensitive in identifying histopathological tissue properties. A P value lower than 0.01, which is often considered in the literature to be the threshold value for declaring that the differences are at a high level of significance, was obtained for each feature considered in the study, see Fig. 6. NAA, tCho group and Lips are F6
interconnected. This interconnectivity gives rise for example to correlations between decreased Cho and Lips and increased NAA in the border region of the tumor. Better differentiation between necrotic, border and high cellularity tumor tissue is obtained when considering sets of features compared to independent features. In Fig. 7, different metabolic sets are chosen to describe the F7
space in which we analyze the GBM data. We see that the Lips-to-tCho metabolite set allows us to better differentiate necrosis from highly cellular tumor tissue, while best separation between all three tissue properties is given by the tCho-to-NAA set and the Lips-to-NAA set.

The most reliable markers for necrosis are lipids. Ex vivo and in vivo studies have further supported this, showing high correlation between the NMR-visible mobile lipids and the percentage of necrosis (8,3,27). Our findings confirm the previously drawn conclusions. For example, we observe increased concentrations of Lips for the cases with predominant necrotic tissue compared to the respective levels in high cellularity and border tumor tissue. Additionally, we show that lipids are sensitive in identifying border tumor tissue as the concentrations of lipids in border regions are almost negligible, and also for separating both highly cellular tumor tissue and border tumor tissue from necrosis. Furthermore, as in (3), we prove the presence of mobile lipids in tumors with no necrosis. For necrosis, the NAA values are almost negligible

ID: jaishankarn | Black Lining: [ON] | Time: 21:41 | Path: N:/3b2/MRMT/Vol00000/100302/APPFile/JW-MRMT100302

J_ID: Z3T Customer A_ID: MRM22619 Cadmus Art: MRM22619 Ed. Ref. No.: 10-11431.R2 Date: 30-August-10 Stage: Page: 7



C O L O R

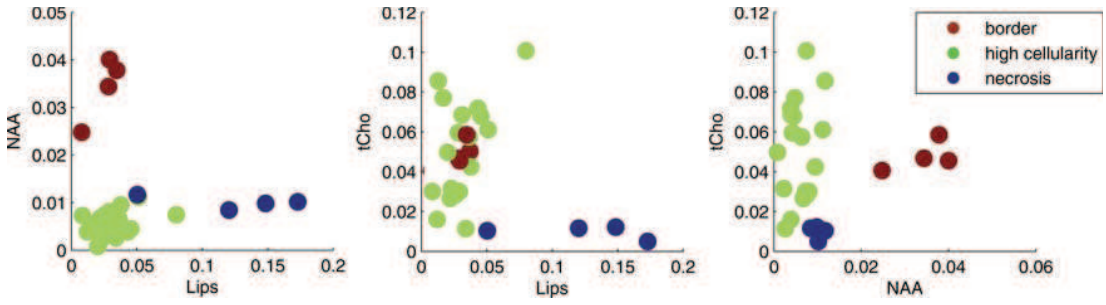
FIG. 6. Comparison plot after performing the Kruskal-Wallis test (*P* value is indicated) and the Tukey's multiple comparison. Differences between the three histopathological tissue properties for (**a**) the metabolites considered in the study and (**b**) for the metabolite ratio values are illustrated.

and the concentrations of tCho are also very low. Having as reference the sum of all the considered metabolites, in necrotic tissue we observe NAA level <20%, while Lip(s) level >60% and Cho(s) level <30%; see Fig. 8.

The three main components of the combined tCho peak observed in gliomas, namely Cho, PCho and GPCho, are generally associated with cell turnover. They are reported elevated in highly cellular tumor tissue and can aid in identifying the malignancy grade (24,28,29). Still, in (30) the authors suggested that the tCho group could not be used to differentiate low grade glioma from high grade glioma. Our results show that degradations in the tCho concentrations are associated with the histopathological tissue property. tCho values are the highest in highly cellular tumor regions and relatively high in border regions. The very low relative tCho concentrations detected for predominantly necrotic tissue (see Fig. 6), can be an effect of dilution of absolute cellular density due to the presence of necrosis (31). Additionally, for the highly cellular tissue, the level of NAA is very low, the Lips are much lower compared to necrotic tissue, but not varying too much from the values reported in border regions. As a conclusion of our results, the Lip(s) level <50%, NAA level <20%, and Cho(s) level >40% in highly cellular areas.

A distinguishable characteristic of border tumor tissue is the high level of NAA, a known marker of normal neuronal function (23). NAA has high sensitivity for identifying border tumor tissue, but also for separating the necrosis from the rest of the other two considered tissue properties, as the values of NAA are very high in border tissue, almost negligible in necrotic tissue compared to border tissue, and a decrease in the NAA peak is observed in highly cellular tissue. As seen in Fig. 8, Lip(s) level <40%, NAA level >20%, Cho(s) level >20% within the border tumor regions.

Creatine (Cr) is typically used as an internal reference. In (30), the ratio of NAA/tCr was reported as significantly



C O L O R

FIG. 7. All GBM cases plotted in the Lips-to-NAA, tCho-to-Lips, and tCho-to-NAA space, respectively.

J_ID: Z3T Customer A_ID: MRM22619 Cadmus Art: MRM22619 Ed. Ref. No.: 10-11431.R2 Date: 30-August-10 Stage: Page: 8

C O L O R

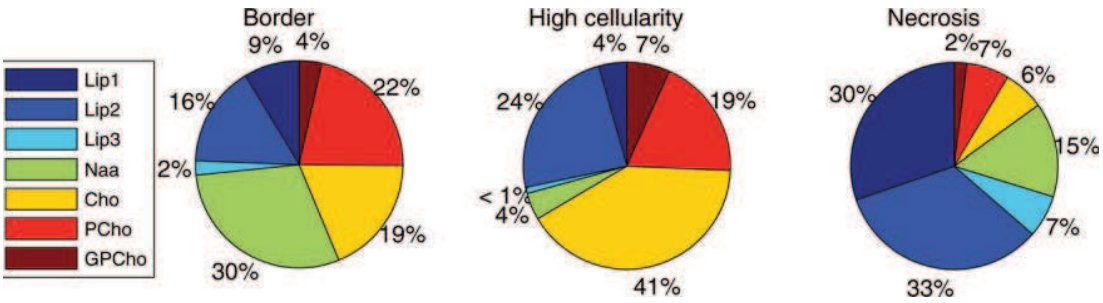


FIG. 8. Metabolites distribution for different histopathological tissue properties. The percentage values reflect the ratio between individual metabolite concentrations and the sum of all the considered concentrations.

decreased in the tumor region compared to the same ratio in normal brain ($P < 0.01$). The tCho/Cr ratio decreases in gliomas with the malignancy of the tumor (32) and may solve some tumor classification problems (7,33). To comply with previous studies, ratios of Lips, tCho and NAA to Cr are considered. We found that in border tissue Lips/Cr ratios are low or very low, the Cho/Cr, PCho/Cr and GPCho/Cr ratios are <1.5 and NAA/Cr is not negligible. For high cellularity, the Lips/Cr ratios are low or very low, the Cho/Cr, PCho/Cr and GPCho/Cr ratios are greater than or close to 1.5 and NAA/Cr is negligible. For necrosis, the NAA/Cr ratios are almost negligible, Cho/Cr values are very low and Lips/Cr values are very high relative to the other two. Still, with any given tumor group, metabolite concentration sets indicate better than ratio sets the predominant histopathological tissue property.

Lactate (Lac) levels are reported in (8) to correlate, for the single patient case studied, with the level of necrosis. Still, some HR-MAS acquisition variables, such as the effects of changing the sample volume in the MAS rotor, snap-freezing the samples, the temperature conditions, could have an influence on the concentration of Lac. Moreover, as shown in (34), due to the unavoidable period of ischemia during the biopsy procedure, Lac would be significantly altered when using HR-MAS. Consequently, Lac was not considered in our study.

Similar metabolic patterns were observed for the considered tissue properties, regardless of the grade of malignancy. The results demonstrate the biological relevance of MRS biomarkers in understanding the biology of the tumor, with potential in improving noninvasive diagnosis and in aiding clinicians in improving diagnosis and treatment and ongoing evaluation of the patients. Even if the diagnosis assignment is progressively improving by implementations of a variety of pattern recognition methodologies (35), still difficulties remain in the grading of glial tumor. This may be due to the fact that the methodologies proposed are not sensitive to the microheterogeneity of the tissue. Commonly, the tumor classification problem is limited to separating between different tumor grades, without considering the contributions of necrotic or normal tissue in the metabolic profile of the spectra under investigation. As it was shown in this study, there is a high variability within the HR-MAS data coming from the same tumor grade group. This intragroup metabolic variability is a consequence of the tumor microheterogeneity, since no biopsy procedure could guarantee the homogeneity of the sample under investigation. Ignoring a first separation between the three histopathological tissue properties will highly affect the performance of any classifier applied on HR-MAS data. Tissue microheterogeneity is expected to be reflected also in the spectral profile of in vivo MRS or MRSI measurements, where one will deal with large voxel volumes (the area under investigation is much larger than with HR-MAS). We believe that our findings could be translated to in vivo studies and, therefore, could aid in the interpretation of low resolution single-voxel MRS and multivoxel MRSI. This is especially supported by previous studies that reported for the metabolites considered here a high correlation between ex vivo and in vivo MRS (34,36,37). Moreover, there are situations in which prior knowledge on the intratumor tissue differences could add to the power of an accurate tumor classification, by improving the identification of the glial tumor grade (6) or in separating glioblastomas from metastasis (38,39).

One should not neglect the fact that the examined tissue samples have variable content of necrotic, border and high cellular tumor tissue, as reported by the histopathology. This characteristic could be observed also with HR-MAS data as some cases were very close to the border between two tissue types. Further studies on tissue source separation and quantification of the contribution (abundance) of each source within each tissue sample are in progress.

CONCLUSIONS

A strong correlation between the histopathological tissue properties and metabolic profiles coming from ex vivo HR-MAS is observed in glial tumors. A clear separation between necrotic tissue, high cellularity tumor tissue and border tumor tissue is obtained regardless of the malignancy grade. The metabolite concentration sets can better differentiate between the considered histopathological tissue properties than the ratios of the metabolites to Cr. We show that the alteration in metabolite concentrations are correlated and interdependent, and representative metabolic tissue models corresponding to each histopathological tissue property could be extracted. Ex vivo HR-MAS can therefore provide relevant metabolic information on the tumor tissue under investigation.

ID: jaishankarn | Black Lining: [ON] | Time: 21:41 | Path: N:/3b2/MRMT/Vol00000/100302/APPFile/JW-MRMT100302

J_ID: Z3T Customer A_ID: MRM22619 Cadmus Art: MRM22619 Ed. Ref. No.: 10-11431.R2 Date: 30-August-10 Stage: Page: 9

Likewise, the adequate agreement between ex vivo metabolic characteristics, obtained from the HR-MAS classification and histopathology results, can aid in the interpretation of in vivo spectra and, therefore, increase their importance in noninvasive brain tumor classification.

ACKNOWLEDGMENTS

Diana M. Sima acknowledges a postdoctoral fellowship from the Foundation for Scientific Research Flanders. The authors thank Daniel Monleon.

REFERENCES

1. Rutter A, Hugenholtz H, Saunders JK, Smith ICP. Classification of brain tumors by ex vivo ^{1}H NMR spectroscopy. J Neurochem 1995; 64:1655–1661.
2. Howe FA, Barton SJ, Cudlip SA, Stubbs M, Saunders DE, Murphy M, Wilkins P, Opstad KS, Doyle VL, McLean MA, Bell BA, Griffiths JR. Metabolic profiles of human brain tumours using quantitative in vivo ^{1}H magnetic resonance spectroscopy. Magn Res Med 2003;49: 223–232.
3. Opstad KS, Bell BA, Griffiths JR, Howe FA. An investigation of human brain tumour lipids by high-resolution magic angle spinning ^{1}H MRS and histological analysis. NMR Biomed 2008;21:677–685.
4. McKnight TR. Proton magnetic resonance spectroscopic evaluation of brain tumor metabolism. Semin Oncol 2004;31:605–617.
5. Negendank WG, Sauter R, Brown TR, Evelhoch JL, Falini A, Gotsis ED, Heerschap A, Kamada K, Lee BC, Mengeot MM, Moser E, Padavic-Shaller KA, Sanders JA, Spraggins TA, Stillman AE, Terwey B, Vogl TJ, Wicklow K, Zimmerman RA. Proton magnetic resonance spectroscopy in patients with glial tumors: a multicenter study. J Neurosurg 1996;84:449–458.
6. Erb G, Elbayed K, Piotto M, Raya J, Neuville A, Mohr M, Maitrot D, Kehrli P, Namer IJ. Toward improved grading of malignancy in oligodendrogliomas using metabolomics. Magn Reson Med 2008;59: 959–965.
7. McKnight TR, Lamborn KR, Love TD, Berger MS, Chang S, Dillon WP, Bollen A, Nelson SJ. Correlation of magnetic resonance spectroscopic and growth characteristics within grades II and III gliomas. J Neurosurg 2007;106:660–666.
8. Cheng LL, Anthony DC, Comite AR, Black PM, Tzika AA, González RG. Quantification of microheterogeneity in glioblastoma multiforme with ex vivo high-resolution magic-angle spinning (HR-MAS) proton magnetic resonance spectroscopy. Neuro Oncol 2000;2:87–95.
9. Andronesi OC, Blekas KD, Mintzopoulos D, Astrakas L, Black PM, Tzika AA. Molecular classification of brain tumor biopsies using solid-state magic angle spinning proton magnetic resonance spectroscopy and robust classifiers. Int J Oncol 2008;33:1017–1025.
10. Tzika AA, Astrakas L, Cao H, Mintzopoulos D, Andronesi OC, Mindrinos M, Zhang J, Rahme LG, Blekas KD, Likas AC, Galatsanos NP, Carroll RS, Black PM. Combination of high-resolution magic angle spinning proton magnetic resonance spectroscopy and microscale genomics to type brain tumor biopsies. Int J Mol Med 2007;20: 199–208.
11. Righi V, Roda JM, Paz J, Mucci A, Tugnoli V, Rodriguez-Tarduchy G, Barrios L, Schenetti L, Cerdan S, Garcia-Martin ML. ^{1}H HR-MAS and genomic analysis of human tumor biopsies discriminate between high and low grade astrocytomas. NMR Biomed 2009;22:629–637.
12. Louis DN, Ohgaki H, Wiestler OD, Cavenee WK.World health organization classification of tumours of the central nervous system.Lyon:IARC;2007; ISBN 9283224302.
13. Laudadio T, Mastronardi N, Vanhamme L, Van Hecke P, Van Hufel P. Improved Lanczos algorithms for blackbox MRS data quantitation. J Magn Res 2002;157:292–297.
14. Poullet JB, Martinez-Bisbal MC, Valverde D, Monleon D, Celda B, Arus C, Van Huffel S. Quantification and classification of high-resolution magic angle spinning data for brain tumor diagnosis. Conf Proc IEEE Eng Med Biol Soc 2007;2007:5407–5410.
15. Hartigan JA, Wong MA. A K-means clustering algorithm. Appl Statistics 1979;28:100–108.
16. Cohen J, Cohen P, West SG, Aiken LS. Applied multiple regression/ correlation analysis for the behavioral sciences. Lawrence Erlbaum Associates; 2003. AQ3
17. Strehl A. Relationship-based clustering and cluster ensembles for high-dimensional data mining, PhD thesis, Austin, 2002.
18. Krzanowski J, Lai YT. A criterion for determing the number of groups in a data set using sum-of-squares clustering. Biometrics 1985;44:23–34.
19. Rousseeuw PJ. Silhouettes: a graphical aid to the interpretation and validation of cluster analysis. J Comp Appl Math 1987;20:53–65.
20. Kaufman L, Rousseeuw PJ. Finding groups in data: an introduction to cluster analysis. New York: Wiley; 1990
21. Tukey JW. Comparing individual means in the analysis of variance. Biometrics 1949;5:99–114.
22. Hollander M, Wolfe DA. Nonparametric statistical methods. New York: Wiley; 1973.
23. Peeling J, Sutherland G. High-resolution ^{1}H NMR spectroscopy studies of extracts of human cerebral neoplasms. Magn Reson Med 1992; 24:123–136.
24. Tedeschi G, Lundbom N, Raman R, Bonavita S, Duyn JH, Alger JR, Di C. Increased choline signal coinciding with malignant degeneration of cerebral gliomas: a serial proton magnetic resonance spectroscopy imaging study. J Neurosurg 1997;87:516–524.
25. Gower JC, Hand DJ. Biplots. London, UK: Chapman & Hall; 1996. ISBN 0412716305.
26. Barba I, Cabañas ME, Arús C. The relationship between nuclear magnetic resonance-visible lipids, lipid droplets, and cell proliferation in cultured C6 cells. Cancer Res 1999;59:1861–1868.
27. Kuesel AC, Sutherland GR, Halliday W, Smith ICP. ^{1}H MRS of high grade astrocytomas: mobile lipid accumulation in necrotic tissue. NMR Biomed 1994;7:149–155.
28. Usenius JP, Vainio P, Hernesniemi J, Kauppinen RA. Choline containing compounds in human astrocytomas studied by ^{1}H NMR spectroscopy in vivo and in vitro. J Neurochem 1994;63:1538–1543.
29. Podo F. Tumour phospholipid metabolism. NMR Biomed 1999;12: 413–439.
30. Tong Z, Yamaki T, Harada K, Houkin K. In vivo quantification of the metabolites in normal brain and brain tumors by proton MR spectroscopy using water as an internal standard. Magn Reson Imaging 2004; 22:735–742.
31. Howe FA, Opstad KS. ^{1}H MR spectroscopy of brain tumours and masses. Nucl Magn Reson Biomed 2003;16:123–131.
32. Stadlbauer A, Gruber S, Nimsky C, Fahlbusch R, Hammen T, Buslei R, Tomandl B, Moser E, Ganslandt O. Preoperative grading of gliomas by using metabolite quantification with high-spatial-resolution proton MR spectroscopic imaging. Radiology 2006;238:958–969.
33. Majos C, Margarida Julia-Sape M, Alonso J, Serrallonga M, Aguilera C, Acebes JJ, Arus C, Gili, K. Brain tumor classification by proton MR spectroscopy: comparison of diagnostic accuracy at short and long TE. Am J Neuroradiol 2004;25:1696–1704.
34. Opstad KS, Wright AJ, Bell BA, Griffiths JR, Howe FA. Correlations between in vivo (1) H MRS and ex vivo (1) H HRMAS metabolite measurements in adult human gliomas. J Magn Reson Imaging 31:289–297.
35. Poullet JB, Sima DM, Van Huffel S. Metabolite quantification in MRS and pattern recognition. Encyclopedia of magnetic resonance. New York: Wiley; 2009. pp 1–9; Lirias number: 229620.
36. Martiinez-Bisbal MC, Martii-Bonmati L, Piquer J, Revert A, Ferrer P, Llacer JL, Piotto M, Assemat O, Celda B. ^{1}H and ^{13}C HR-MAS spectroscopy of intact biopsy samples ex vivo and in vivo ^{1}H MRS study of human high grade gliomas. NMR Biomed 2004;17:191–205.
37. Celda B, Monleón D, Martínez-Bisbal MC, Esteve V, Martínez-Granados V, Pinero E, Ferrer R, Piquer J, Martí-Bonmati L, Cervera J, López-Guerrero LA. New trends in cancer for the 21st century. Adv Exp Med Biol 2006;587:285–302.
38. Fan G, Sun B, Wu Z, Guo Q, Guo Y. In vivo single-voxel protonMR spectroscopy in the differentiation of high-grade gliomas and solitary metastases. Clin Radiol 2004;59:77–85.
39. Luts J, Laudadio T, Martinez-Bisbal MC, Van Cauter S, Molla E, Piquer J, Suykens JAK, Himmelreich U, Celda B, Van Huffel S. Differentiation between brain metastases and glioblastoma multiforme based on MRI, MRS and MRSI. In: Proceedings of the 22nd IEEE International Symposium on Computer-Based Medical Systems (CBMS), Albuquerque, New Mexico; August 2009. pp 1–8. AQ4

ID: jaishankarn | Black Lining: [ON] | Time: 21:41 | Path: N:/3b2/MRMT/Vol00000/100302/APPFile/JW-MRMT100302